Proc. 25th Winter Workshop on
Nuclear Dynamics (2009) 000–000

25th Winter Workshop
on Nuclear Dynamics
Big Sky, Montana, USA
February 1–8, 2009

Enhanced Direct Photon Production in Au+Au Collisions at $\sqrt{s_{NN}} = 200$ GeV in PHENIX

S. Bathe[1] for the PHENIX collaboration

[1] RIKEN-BNL Research Center
Brookhaven National Laboratory
Upton NY 11973, USA

Abstract. The production of electron pairs with p_T between 1 and 5 GeV/c and $m < 300$ MeV has been measured at mid-rapidity in $\sqrt{s_{NN}} = 200$ GeV $p+p$ and Au+Au collisions by the PHENIX experiment at RHIC. A significant excess above the hadronic background was observed in both $p+p$ and Au+Au collisions. Treating the excess as internal conversion of direct photons, the direct photon yield in Au+Au was found to be enhanced compared to the binary-scaled $p+p$ yield. The enhancement is consistent with an exponential inverse slope of 221±23±18 MeV and predictions from hydrodynamical models with initial temperature between 300 and 600 MeV at formation times of 0.6–0.15 fm/c.

Keywords: direct photons, nucleus-nucleus collisions, $p+p$ collisions, heavy ion, electron pair production, PHENIX, RHIC
PACS: 13.85.Qk, 13.20.Fc, 13.20.He, 25.75.Dw

1. Introduction

A multitude of results from the Relativistic Heavy Ion Collider (RHIC) at Brookhaven National Laboratory (BNL) indicates the creation of a high-density, thermalized medium in ultra-relativistic collisions of heavy ions [1]. Such a medium is expected to radiate thermal photons [2], which, once produced, leave the medium unscathed. Thermal photons from the partonic phase of the collision are predicted to dominate the direct photon spectrum in the transverse momentum (p_T) range of 1–3 GeV/c as illustrated in Fig. 1 [2]. However, here direct photons are submerged in a background of hadronic decay photons, mainly from the π^0 and η. This background constitutes a major experimental challenge in the conventional, calorimeter-based measurement. It can be overcome, though, by measuring low-mass electron pairs in a mass range where electron pairs from the π^0 Dalitz decay do not contribute [3].

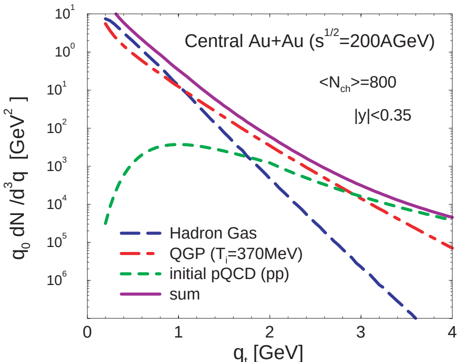

Fig. 1. Direct photon sources at RHIC [2].

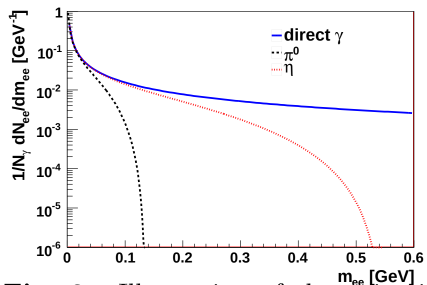

Fig. 2. Illustration of the pair yield mass dependence for direct photons as well as for π^0 and η Dalitz pairs.

The electron-pair yield above the hadronic background can be treated as internal conversion of direct photons [4].

2. Internal Conversion Method

Any source of high-energy photons also emits virtual photons with very low mass [4]. Those virtual photons then convert to low-mass e^+–e^- pairs, which can be measured (*Internal Conversion Method*). The pair yield per direct photon falls with the pair mass as:

$$\frac{d^2 n_{ee}}{dm} = \frac{2\alpha}{3\pi}\frac{1}{m}\sqrt{1 - \frac{4m_e^2}{m^2}}\left(1 + \frac{2m_e^2}{m^2}\right) S dn_\gamma. \tag{1}$$

Here α is the fine structure constant, m_e and m are the masses of the electron and the e^+–e^- pair, respectively, and S is a process dependent factor that goes to 1 as $m \to 0$ or $m \ll p_T$. Equation 1 also describes the relation between photons from hadron decays (e.g. $\pi^0, \eta \to \gamma\gamma$, and $\omega \to \gamma\pi^0$) and e^+–e^- pairs from Dalitz decays ($\pi^0, \eta \to e^+$–$e^-\gamma$ and $\omega \to e^+$–$e^-\pi^0$). For π^0 and η, the factor S is given by $S = |F(m^2)|^2(1 - \frac{m^2}{M_h^2})^3$ [5], where M_h is the meson mass and $F(m^2)$ is the form factor. Figure 2 illustrates the pair yield mass dependence for direct photons as well as for π^0 and η Dalitz pairs. The cut-off of the π^0 pairs at the π^0 mass can be exploited to increase the signal-to-background ratio from 10%, where it is comparable to the systematic uncertainty and therefore not significant, to 50%, making a significant measurement possible. Since the measurement at low p_T is systematics limited, the simultaneous reduction in statistical significance is an acceptable trade-off[1].

[1] There are about 0.001 virtual photons with $m_{ee} > M_{\pi^0}$ for every real photon.

3. Data Set And Backgrounds

The analysis is based on two data sets: Au+Au at $\sqrt{s_{NN}} = 200$ GeV acquired in 2004 consisting of 0.8 billion minimum bias events (4.9 pb^{-1} $p+p$ equivalent); $p+p$ at the same cms energy acquired in 2005 with 2.25 pb^{-1}. Charged tracks were measured with the Drift Chamber and Pad Chamber of the PHENIX [6] Central Arms covering $|\eta| < 0.35$ and $\Delta\phi = 2 \times \pi/2$ and identified as electrons with the Ring Imaging Čerenkov Detector (RICH) and Electromagnetic Calorimeter (EMCal). Material conversion pairs were removed by a cut on the orientation of the pair plane with respect to the magnetic field. Combinatorial background was removed by an event mixing technique, accurate to 0.25% systematic uncertainty in Au+Au.

There is additional correlated background from two sources: *cross pairs* with one electron/positron from either virtual photon in a double-Dalitz decay; *jet pairs* from two different Dalitz decays within the same jet or from back-to-back jets. These contributions can be well understood in a Monte Carlo calculation and have been subtracted.

4. Signal Extraction

After subtraction of the combinatorial background and the cross and jet pairs, the pair mass spectrum is compared to a "cocktail" of known hadronic sources [7, 8].

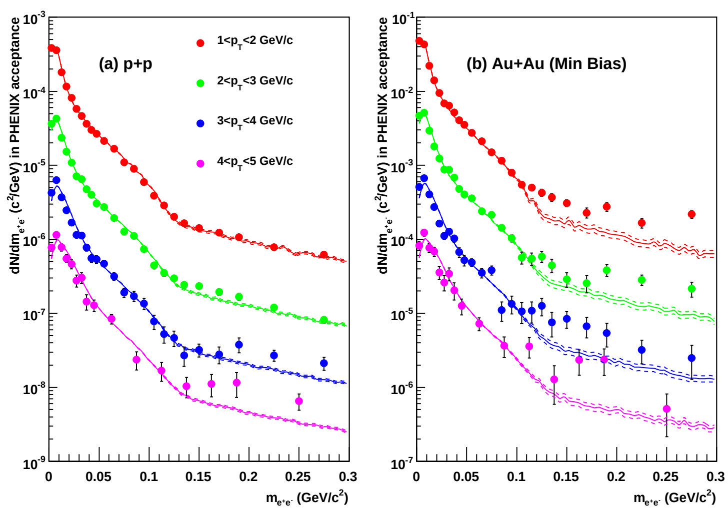

Fig. 3. Pair mass spectra for data (points) and hadronic cocktail (lines) in the PHENIX acceptance for different p_T intervals for $p+p$ (left) and Au+Au (right) [3].

Figure 3 shows this comparison for different p_T intervals for both $p+p$ and Au+Au. The cocktail is normalized to the data for $m < 30$ MeV, where the π^0 Dalitz decay dominates the yield. The "knee" at 100 MeV comes from the π^0 cut-off leading to the 80% background reduction mentioned above.

In $p + p$, the pair yield is consistent with the hadronic background for the lowest p_T interval. At higher p_T a small excess is visible for $m > m_{\pi^0}$. In Au+Au a much larger excess appears at all p_T, indicating an enhanced production of virtual photons[2].

To quantify the direct photon fraction, the mass spectrum is fit with a two-component function $f(m_{ee}) = (1-r)f_c(m_{ee}) + rf_{dir}(m_{ee})$ as illustrated in Fig. 4. Here $f_c(m_{ee})$ is the shape of the cocktail mass distribution (shown in Fig. 3), $f_{dir}(m_{ee})$ is the expected shape of the direct photon internal conversion, and r is the fit parameter. Both $f_c(m_{ee})$ and $f_{dir}(m_{ee})$ are separately normalized to the data for $m_{ee} < 30$ MeV/c^2, where their shapes are nearly identical. This preserves the meaning of r as the *real* direct photon fraction. From the agreement between

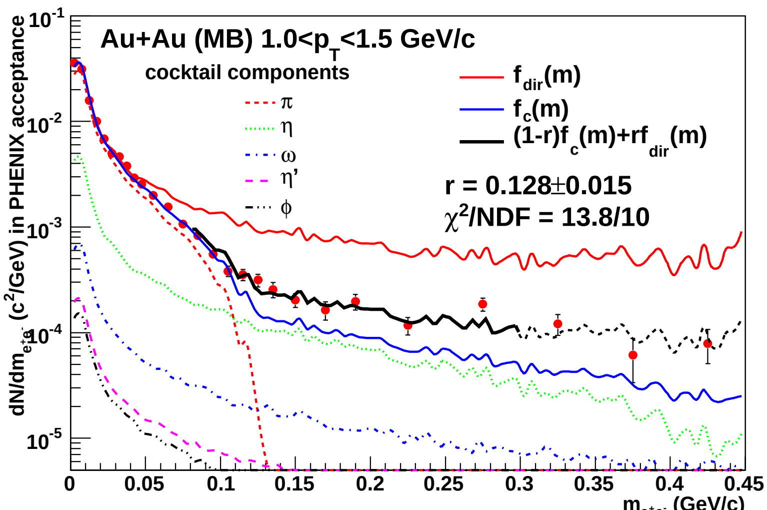

Fig. 4. Illustration of two-component fit to the mass distribution [3].

data and fit it can be concluded that the data matches the expected shape for direct photons.

The so extracted direct photon fraction, r, is plotted as a function of p_T in Fig. 5. While in case of $p + p$ the direct photon fraction is consistent with pQCD, for Au+Au r is enhanced above pQCD.

As this measurement is based on shape differences to extract the direct photon fraction, the η/π^0 ratio is the largest source of systematic uncertainty. This results

[2]This excess is in a different kinematic region (higher p_T, lower mass) than the low-mass enhancement reported in [7], which is expected to be dominated by the hadronic gas phase.

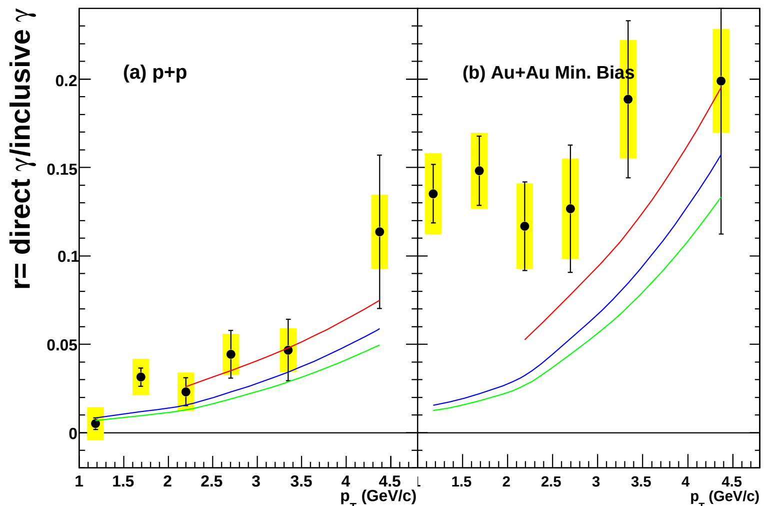

Fig. 5. Direct photon fraction, r, as a function of p_T for $p+p$ and Au+Au events compared to a pQCD calculation for three different scales. In the case of Au+Au the pQCD result is scaled by the nuclear overlap function, T_{AA} [3].

in a 7% uncertainty in $p+p$ and 17% in Au+Au. Other sources contribute only a few percent as the cocktail is normalized to the data and no absolute normalization is required.

In the next step, r is converted into the direct photon yield as $dN^{dir}(p_{\mathrm{T}}) = r \times dN^{incl}(p_{\mathrm{T}})$. The inclusive photon yield for each p_{T} bin is determined by $dN_{\gamma}^{incl} = N_{ee}^{data} \times (dN_{\gamma}^{c}/N_{ee}^{c})$, where N_{ee}^{data} and N_{ee}^{c} are the measured and the absolutely normalized cocktail e^{+}–e^{-} pair yields, respectively, both for $m_{ee} < 30$ MeV/c^2; and dN_{γ}^{c} is the yield of photons from the cocktail. Here we use the fact that the ratio of the photon yield to the e^{+}–e^{-} pair yield for $m_{ee} < 30$ MeV/c^2 calculated from Eq. 1 is the same within a few percent for any photon source. The systematic uncertainty of γ^{incl} is 14% from the e^{+}–e^{-} pair acceptance.

5. Results

Figure 8 shows the invariant yield of direct photons as a function of p_T for $p+p$ and three different centrality classes in Au+Au. The $p+p$ data is again compared to the pQCD calculation. The calculation is consistent with the data for $p_T > 2$ GeV. A modified power law, $A_{pp}(1+p_T^2/b)^{-n}$, fits the data over the entire p_T range.

5.1. Significance of the Modified Power Law

The modified power law appears to yield an at least as good description of the data at low p_T as the pQCD calculation. What is the significance of this observation? It is obvious that the power-law behavior of hard scattering has to break down for $p_T \rightarrow 0$. For hadrons, soft production sets in with an exponential slope. This is illustrated in Fig. 6, which shows a parameterization of π^0 production in $p+p$ [9]. The parameterization is the sum of a power law and an exponential with a Woods-Saxon transition between the two. The two functions are shown separately. The exponential dies out at high p_T while the power law diverges at low p_T. The hard-scattering contribution can be understood as the difference between the data parameterization and the exponential contribution. One can see that it flattens out towards low p_T, deviating from the power law. This flattening corresponds to an onset of hard scattering as illustrated by the ratio of the hard scattering contribution to the power law.

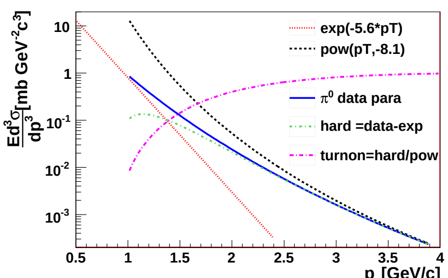

Fig. 6. Parameterization of π^0 production in $p+p$ [9] and its various contributions (for details see text).

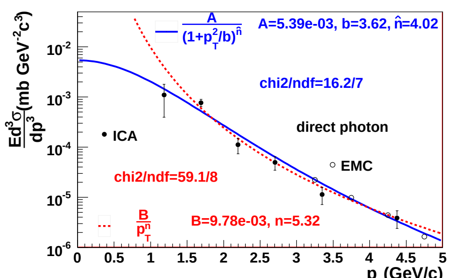

Fig. 7. Fit of direct photon cross section with both a power law and a modified power law.

This onset is not directly observable for hadrons as the production at low p_T is dominated by soft physics. Direct photons, however, are only produced in hard scatterings. This makes the onset of hard scattering at low p_T directly measurable. The onset has also been measured in Drell-Yan production [10].

To evaluate the statistical significance of the onset, the PHENIX data were fitted with both a power law and a modified power law. As shown in Fig. 7, the modified power law yields a smaller reduced χ^2 than the pure power law.

5.2. Au+Au Enhancement

For $1 < p_T < 3$ GeV, the direct photon invariant yield in Au+Au is enhanced above the T_{AA}-scaled modified power law that was fit to the $p+p$ data (Fig. 8). It can be well described, however, if an exponential is added. The resulting fit yields negative inverse exponential slopes of about 220 MeV[3]. If the medium were static, T could

[3] If the $p+p$ data are fit with a pure power law, T increases by 24 MeV in central events.

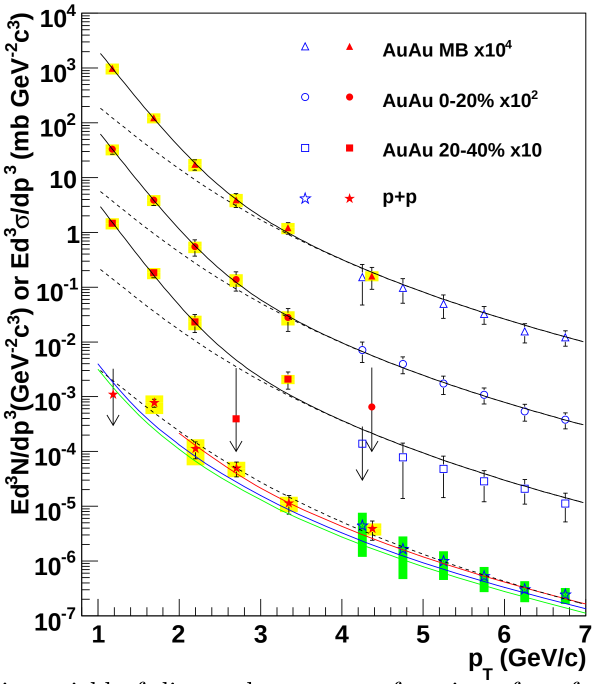

Fig. 8. Invariant yield of direct photons as a function of p_T for $p+p$ and three different centrality classes in Au+Au (solid symbols). The result of an earlier EMCal measurement is also shown (open symbols) [11, 12]. The $p+p$ data is compared to a pQCD calculation shown as three lines for different scales. The dashed line is a fit of a modified power law to the $p+p$ data. The Au+Au data are compared to the T_{AA}-scaled $p+p$ fit (dashed line). The solid line shows the result of a fit where an exponential is added to the T_{AA}-scaled $p+p$ fit [3].

be interpreted as its temperature. For a more realistic temperature estimate, the data is compared to hydrodynamical models. Models that fit the data assume initial temperatures, T_i, between 300 and 600 MeV at formation times, τ_0, between 0.6 and 0.15 fm/c, where the temperature and the formation time are anti-correlated. The 221 ± 23(stat.) $\pm$ 18(sys.)MeV obtained from the data alone serves as a lower limit. Even the lower limit, though, lies above the critical temperature predicted by lattice calculations.

6. Conclusion

An excess of low-mass e^+–e^- pairs above the hadronic background was observed at intermediate p_T (1 GeV $< p_T <$ 5 GeV) for both $p+p$ and Au+Au collisions. The

excess can be understood as the internal conversion of direct photons and shows the expected $1/m$ dependence. In $p+p$, the direct photon yield is consistent with the result of a pQCD calculation. In Au+Au, the yield is much larger. It is enhanced above the binary-scaled $p+p$ yield, represented by a modified power law fit to the $p+p$ data and scaled by T_{AA}. The Au+Au yield can be well described if an exponential is added to the binary-scaled $p+p$ fit. The negative inverse slope of the exponential is 221 $\pm$ 23 (stat.) $\pm$ 18 (sys.) MeV in central Au+Au. For a static medium, this could be interpreted as the temperature. For an expanding medium, it serves as a lower limit of the temperature. It is well above the critical temperature of about 170 MeV. Hydrodynamical models that fit the data assume initial temperatures, T_i, between 300 and 600 MeV at formation times, τ_0, between 0.15 and 0.6 fm/c. Together with the earlier WA98 measurement [13], this result can be interpreted as the first experimental evidence that strongly interacting matter can exceed the Hagedorn temperature of 170 MeV [14].

Acknowledgments

I thank the RIKEN-BNL Research Center for supporting my work and the DOE for operating RHIC and PHENIX.

References

1. K. Adcox et al., *Nucl. Phys.* **A757** (2005) 184.
2. S. Turbide, R. Rapp and C. Gale, *Phys. Rev.* **C69** (2004) 014903.
3. A. Adare et al. ArXiv:0804.4168[nucl-ex] (2008).
4. J. H. Cobb et al., *Phys. Lett.* **B78** (1978) 519.
5. L. G. Landsberg, *Phys. Rept.* **128** (1985) 301.
6. K. Adcox et al., *Nucl. Instrum. Meth.* **A499** (2003) 469.
7. S. Afanasiev et al. ArXiv:0706.3034[nucl-ex] (2007).
8. A. Adare et al., *Phys. Lett.* **B670** (2009) 313.
9. S. S. Adler et al., *Phys. Rev. Lett.* **98** (2007) 172302.
10. A. S. Ito et al., *Phys. Rev.* **D23** (1981) 604.
11. S. S. Adler et al., *Phys. Rev. Lett.* **94** (2005) 232301.
12. S. S. Adler et al., *Phys. Rev. Lett.* **98** (2007) 012002.
13. M. M. Aggarwal et al., *Phys. Rev. Lett.* **85** (2000) 3595.
14. S. C. Frautschi, *Phys. Rev.* **D3** (1971) 2821.